



Apolipoprotein M delays the development of atherosclerosis by regulating autophagy and mitochondrial function

Yuanping Shi¹, Shuang Yao¹, Binhua Jiang², Jun Zhang¹, Mingjun Cao³, Jing Wu¹, Lu Zheng¹, Ning Xu⁴, Xiaoying Zhang^{5*}, Guanghou Shui^{3*}, Guanghua Luo^{1*}

¹Clinical Medical Research Center, the Third Affiliated Hospital of Soochow University, Changzhou, China; ²Lipidall Technologies Company Limited, Changzhou, China; ³Institute of Genetics and Developmental Biology, Chinese Academy of Sciences, Beijing, China; ⁴Section of Clinical Chemistry and Pharmacology, Institute of Laboratory Medicine, Lunds University, Lund, Sweden; ⁵Department of Cardiothoracic Surgery, the Third Affiliated Hospital of Soochow University, Changzhou, China

Contributions: (I) Conception and design: Y Shi, G Luo; (II) Administrative support: X Zhang, G Shui, N Xu; (III) Provision of study materials or patients: G Shui, S Yao, J Zhang; (IV) Collection and assembly of data: Y Shi, S Yao, M Cao, J Wu, L Zheng; (V) Data analysis and interpretation: Y Shi, B Jiang; (VI) Manuscript writing: All authors; (VII) Final approval of manuscript: All authors.

*These authors contributed equally to this work.

Correspondence to: Xiaoying Zhang, MD. Department of Cardiothoracic Surgery, the Third Affiliated Hospital of Soochow University, No. 185, Juqian Street, Changzhou 213003, China. Email: zhangxy6689996@163.com; Guanghou Shui, PhD. Institute of Genetics and Developmental Biology, Chinese Academy of Sciences, No. 2, Courtyard 1, Beichen West Road, Chaoyang District, Beijing 100101, China. Email: ghshui@genetics.ac.cn; Guanghua Luo, MD. Clinical Medical Research Center, the Third Affiliated Hospital of Soochow University, No. 185, Juqian Street, Changzhou 213003, China. Email: shineroar@163.com.

Background: Apolipoprotein M (ApoM), a protein component of lipoproteins, is closely related to the development of atherosclerosis, but the specific mechanism remains elusive. Mitochondrial DNA damage can contribute to atherosclerosis, so this study was designed to investigate whether ApoM influences the structure and function of mitochondria during the progression of atherosclerosis and to explore the underlying mechanism.

Methods: Atherosclerosis models were established in male ApoM-deficient (*ApoM*^{-/-}) and wild-type (*ApoM*^{+/+}) C57BL/6 mice fed a high-fat diet (HFD), and the development of atherosclerosis was verified by en face analysis of the aorta and Masson's trichrome staining. We utilized transmission electron microscopy (TEM) to examine the ultrastructure of the aorta, its endothelial cells and EA.hy926 cells. Mass spectrometry-based lipidomics was performed to measure lipidomes in the serum and liver tissue of *ApoM*^{-/-} mice. In EA.hy926 cells, we modulated the levels of autophagy and ApoM expression, and investigated the mechanism by which ApoM influences the pathogenesis of atherosclerosis through western blotting, JC-1 staining, flow cytometry, and Seahorse extracellular flux analysis.

Results: In *ApoM*^{-/-} mice fed an HFD, atherosclerotic markers such as aortic lipid accumulation, fibrosis, endothelial cell oedema, and mitochondrial swelling were observed, indicating early atherosclerotic development. Lipidomic analysis revealed that ApoM deficiency might lead to impaired autophagy and mitochondrial dysfunction. In EA.hy926 cells, overexpression of ApoM not only activated autophagy but also improved mitochondrial structure. Moreover, ApoM decreased the mitochondrial membrane potential ($\Delta\Psi_m$) of EA.hy926 cells, which was further reduced by autophagy activation. Additionally, overexpression of ApoM in EA.hy926 cells, which have a low basal metabolism and primarily rely on glycolysis for energy, significantly reduced basal mitochondrial respiration and adenosine triphosphate (ATP) production, suggesting that ApoM can facilitate mitochondrial fission.

Conclusions: ApoM exerts atheroprotective effects by promoting autophagy and regulating mitochondrial dynamics, thereby maintaining mitochondrial integrity and function. This study provides novel insights into the mechanisms underlying the protective role of ApoM in atherosclerosis and highlights its potential as a therapeutic target for cardiovascular diseases.

Keywords: Apolipoprotein M (ApoM); atherosclerosis; mitochondria; autophagy; lipid metabolism

Submitted Nov 25, 2024. Accepted for publication Apr 09, 2025. Published online Apr 22, 2025.

doi: 10.21037/cdt-2024-614

View this article at: <https://dx.doi.org/10.21037/cdt-2024-614>

Introduction

Atherosclerosis is a chronic inflammatory vascular disease that is mainly caused by disordered lipid metabolism and the deposition of foam cells that engulf large amounts of lipids. Atherosclerosis is the pathological basis of a series of ischemic cardiovascular and cerebrovascular diseases (1,2) and is the main cause of cardiovascular and cerebrovascular

events and deaths worldwide. It poses a great threat to human life and health. The pathogenesis and pathological process of atherosclerosis is very complex. Disordered lipid metabolism leads to a series of pathophysiological changes in the arterial wall (3,4), and the activation of immunity/inflammation in the vascular wall is considered one of the key factors in the occurrence and development of atherosclerosis (5). High-density lipoprotein (HDL) and low-density lipoprotein (LDL), which are important substances in lipid metabolism, are closely associated with the occurrence of atherosclerosis (6). Apolipoprotein is the protein component of lipoproteins and plays an important role in lipoprotein metabolism and its physiological function. Apolipoprotein M (ApoM) is a human apolipoprotein isolated and cloned from chylomicron in 1999 that mainly exists in HDL (7). Polarized endothelial cells lining the blood brain barrier can also express ApoM and secrete this protein into both the brain and the blood compartment (8). Previous studies have shown that ApoM itself can increase HDL levels or bind to Sphingosine-1-Phosphate (S1P) as a complex to play a role in inhibiting atherosclerosis (9-11). ApoM features a hydrophobic binding pocket primarily responsible for carrying S1P (8). ApoM binds to and holds S1P, thereby safeguarding endothelial cells and preserving vascular integrity (12).

Zhang *et al.* (13) found that the autophagy disorder caused by ApoM deficiency plays an important role in liver lipid metabolism disorder. Guo *et al.* (14) showed that ApoM could reduce the cardiotoxicity of doxorubicin and lysosome damage and maintain myocardial autophagic flux. Autophagy is a process in eukaryotic cells with the purpose of achieving self-protection by degrading damaged organelles and proteins that exhibits low levels of activation in cells under normal physiological conditions (15). A change in autophagy in endothelial cells, macrophages, and smooth muscle cells is one of the factors in the development of atherosclerosis, and endothelial autophagy often protects against the development of atherosclerosis (16,17). However, whether the involvement of ApoM in the pathogenesis of atherosclerosis is related to the autophagy-lysosomal pathway has not been studied.

Highlight box

Key findings

- The apolipoprotein M (ApoM)-deficient mice on a high-fat diet (HFD) exhibited significant early signs of atherosclerosis, including increased aortic lipid accumulation, fibrosis, endothelial cell edema, and mitochondrial swelling, indicating a progression of atherosclerotic changes.
- Mass spectrometry-based lipidomics revealed that ApoM deficiency is associated with impaired autophagy and mitochondrial dysfunction.
- ApoM overexpression decreased the mitochondrial membrane potential in EA.hy926 cells, which was further reduced by the activation of autophagy. This suggests that ApoM may facilitate mitochondrial fission, a process critical for mitochondrial health and function.

What is known and what is new?

- Previous research has highlighted ApoM is linked to atherosclerosis, influencing lipid metabolism and endothelial function. Further research is needed to elucidate these mechanisms.
- This study adds to existing knowledge by suggesting that ApoM may protect against atherosclerosis by promoting autophagy and regulating mitochondrial dynamics, thereby preserving mitochondrial function and integrity of endothelial cells.

What is the implication, and what should change now?

- The findings of this study highlight the critical role of ApoM in regulating autophagy and mitochondrial dynamics, suggesting its potential as a therapeutic target for atherosclerosis.
- To leverage these insights, clinical strategies should focus on enhancing ApoM expression or function to improve mitochondrial integrity and autophagy in endothelial cells. Additionally, further research is needed to explore ApoM-based therapies and biomarkers for early atherosclerosis detection and intervention, ultimately aiming to reduce cardiovascular disease risk and improve patient outcomes.

Mitochondria are the centers of energy supply and metabolism in cells, and their morphology and quantity can change dynamically. Mitochondria can be renewed by moving in the cytoplasm and constantly undergoing fission and fusion to form organelle groups. Mitochondrial DNA damage can cause atherosclerosis (18,19). Pei *et al.* (20) found abnormal changes in renal mitochondrial damage and endoplasmic reticulum stress in ApoM-deficient mice compared with wild-type mice. However, whether ApoM is involved in cardiovascular diseases, especially atherosclerosis, and is related to the mitochondrial pathway has not been reported.

Our research group demonstrated dysregulated lipid metabolism in ApoM-knockout mice through lipidomics analysis, identified the types of lipids that were significantly affected by ApoM-knockout, and analyzed the possible reasons for the decrease in liver lipid secretion into the circulation (21). Subsequently, we showed that the mitochondrial function of ApoM-deficient hepatoma cells was abnormal (21). Recently, we further compared and analyzed the lipidomics data and found that lysobisphosphatidic acid (LBPA), a characteristic marker of the lysosomal degradation pathway, was decreased in the serum of ApoM-knockout mice and in ApoM-KO SMMC-7721 cells, whereas acylcarnitine, a marker of mitochondrial overload, was significantly increased in serum. These findings suggest that the loss of ApoM expression can lead to a decline in autophagy and mitochondrial dysfunction. However, the relationship between ApoM expression, autophagy status, mitochondrial function, and atherosclerosis is not clear. In this study, to further understand the mechanism of abnormal ApoM expression in the development of atherosclerosis, we constructed an ApoM-knockout mouse atherosclerosis model and an EA.hy926 endothelial cell line overexpressing ApoM, regulated the autophagy level of endothelial cells, and examined mitochondrial structure and function to provide a new target and theoretical basis for clinical atherosclerosis disease monitoring, diagnosis, and treatment. We present this article in accordance with the ARRIVE reporting checklist (available at <https://cdt.amegroups.com/article/view/10.21037/cdt-2024-614/rc>).

Methods

Animal studies

Animals and experimental groupings

The mice were obtained from the Model Animal Research

Center of Nanjing University (China). The construction of C57BL/6 *ApoM*^{-/-} mice and their genotype identification were detailed in our previous paper (22). An experimental design assistant (<https://eda.nc3rs.org.uk/eda/login/auth>) was used to calculate the power calculator. The power of the experiment was set to 80%. Totals of 12 male C57BL/6 *ApoM*^{+/+} mice and 12 male C57BL/6 *ApoM*^{-/-} mice were fed a normal diet (ND) and a high-fat diet (HFD) from 6 weeks of age. The mice were randomly divided into 4 groups using a computer-generated random number sequence, with 6 mice in each group: *ApoM*^{+/+} mice in the ND group, *ApoM*^{-/-} mice in the ND group, *ApoM*^{+/+} mice in the HFD group, and *ApoM*^{-/-} mice in the HFD group. The mice in the HFD group were fed an HFD for 6 months. The high-fat formula consisted of 10% lard, 10% milk powder, 2% cholesterol, 0.2% sodium cholate, and 77.8% basic feed (Shuangshi Laboratory Animal Feed Technology Co Ltd., Suzhou, China). The mice were housed in the specific-pathogen-free (SPF) laboratory of the Experimental Animal Center of Soochow University (Suzhou, China), with an ambient temperature controlled at 22±2 °C, humidity maintained between 40–60%, and a 12:12-hour light-dark cycle. The maximum caging density was set at 5 mice per cage. The mice had free access to water and food. The animal experiment was approved by the Ethics Committee of Soochow University. The experimental design and implementation plan of this study fully considered the principles of safety and fairness, as well as the requirements of animal welfare and national animal experiment management and ethics. A protocol was prepared before the study without registration.

Mouse sampling procedures

The mice from the four groups were operated on in rotation to ensure that the interval time for each step was consistent, and the experiment was conducted using a double-blind method. The mice were anaesthetized by an intraperitoneal injection of 10% chloral hydrate after being fed and sacrificed. Whole blood was collected in a vacuum blood collection tube, and serum was separated by centrifugation at 4,000 rpm for 5 minutes. Serum and the right lobe of the liver were collected for lipidomics analysis. Other tissues were harvested, 5 mL of saline was injected twice into the apex of the heart to flush the heart and aorta, 10% formalin was injected to fill the whole aorta, and the aorta was fixed for several minutes. The spine was separated, other tissues and organs were removed, the excess tissue outside the aortic adventitia was carefully removed, the heart was cut

and fixed separately, and follow-up staining was performed. Aortic arches with a length of 2–3 mm in each group were immersed in an electron microscopy fixative for subsequent transmission electron microscopic (TEM) observation.

En face staining and measuring the area of the aorta

The aorta was dissected, and a small incision was made using scissors. A sharp surgical blade was employed to cut vertically and longitudinally from the middle of the blood vessel. The vessel was then flattened onto filter paper and then stained according to the conventional en face staining protocol. MicroTek Scan Wizard 5.0 (Microtek International, New Delhi, India) was used to scan the mounted sample, and ImageJ win32 software (National Institutes of Health, Bethesda, MD, USA) was used to measure the staining area.

Masson's trichrome staining of the aortic root

The whole tissue of the joint between the heart and aorta was preserved and fixed in 10% formalin solution. Then, the tissue was trimmed, paraffin sections were prepared, and Masson collagen fiber staining was performed according to conventional methods. Histopathological observation of aortic specimens was performed under an optical microscope, and blue collagen fibers and red muscle fibers were observed. The results were evaluated by pathologists.

TEM analysis of the aorta

The aorta was fully fixed after being excised, and the sections were prepared by the conventional method. The production of TEM samples was supported by Wuhan Servicebio Biotechnology Co. Ltd. (Wuhan, China). The degree of injury in the whole aorta and endothelial cells and morphological changes in each organelle were observed.

Lipidomics analysis

Lipidomics analysis was performed by LipidAll Technologies Company Limited (Changzhou, China) as described previously (23). Lipids were extracted from the serum and livers of mice by the modified Bligh and Dyer method (24). Liquid chromatography-mass spectrometry (LC-MS) analysis was performed on an Exion ultra-performance liquid chromatograph (UHPLC; Sciex, Framingham, MA, USA) coupled to a Sciex QTRAP 6500 Plus. Further details of the lipidomics analysis can be found in previous publications by our group.

Cell experiment

Cell cultures

EA.hy926 cells were procured from the American Type Culture Collection (ATCC, Manassas, VA, USA) and cultured in Dulbecco's modified Eagle's medium supplemented with 10% fetal bovine serum (FBS) in a 60 mm dish. The SMMC-7721 cell line, a human hepatoma cell line, was obtained from the cell bank of the Chinese Academy of Sciences and authenticated by short tandem repeat sequence analysis. The cells were propagated in Roswell Park Memorial Institute (RPMI) 1640 medium containing 10% FBS. Our group established the ApoM-knockout (ApoM-KO) SMMC-7721 cell line using the CRISPR/Cas9 system (21).

Construction of ApoM-overexpressing EA.hy926 cells

EA.hy926 cells were infected with the lentivirus. Upon successful infection, green fluorescent protein (GFP) exhibited green fluorescence, and it was verified that ApoM expression significantly increased, as detailed in our previously published article (25).

Western blot analysis

Proteins were extracted from the negative control and EA.hy926 cells overexpressing ApoM according to the procedure of the total protein extraction kit (KeyGen Biotech Co Ltd., Nanjing, China), bicinchoninic acid (BCA) protein quantitation (BestBio, Shanghai, China). The samples were loaded on 15% gels, transferred to a polyvinylidene fluoride (PVDF) membrane and incubated with antibodies against the autophagy marker protein microtubule-associated protein 1 light chain 3 (LC3B) (1:3,000; ABclonal, Wuhan, China), P62 (1:2,000; Proteintech, Rosemont, IL, USA) and β -actin (1:1,000; Cell Signaling Technology, Danvers, MA, USA) overnight at 4 °C. After incubation in enhanced chemiluminescence (ECL) luminescence solution (Thermo Fisher Scientific, Waltham, MA, USA), the signals were observed on a chemiluminescence imaging system (ChemiScope 3300 mini; Shanghai Qinxiang, Shanghai, China). Quantity One software version 4.6.2 (Bio-Rad Laboratories, Inc., Hercules, CA, USA) was used to determine the protein expression of LC3B, P62, and β -actin.

TEM

EA.hy926 cells were divided into 6 groups: the untreated

EA.hy926 cell group, the lentivirus-infected negative control group, the ApoM-overexpressing EA.hy926 cell group, the negative control EA.hy926 cells treated with 20 nM rapamycin (RAPA), an autophagy agonist for 24 hours group, the ApoM-overexpressing EA.hy926 cells treated with 20 nM RAPA for 24 hours group, and the ApoM-overexpressing EA.hy926 cells treated with 1 mM 3-methyladenine (3-MA) for 24 hours group. The cells were seeded in a 100 mm culture dish, the culture medium was removed, and the cells were fixed in 2% glutaraldehyde electron microscopy fixative. The cells were gently scraped off and collected in EP centrifuge tubes and centrifuged at 1,000 rpm for 5 minutes to remove the supernatant, after which 1 mL of fresh 2% glutaraldehyde was added, and the cells were fixed at room temperature in the dark for 20 minutes and centrifuged at 1,000 rpm for 5 minutes to remove the supernatant. Then, 1 mL of fresh 2% glutaraldehyde was added to fix the samples at 4 °C overnight. The mung bean-size precipitate cell group was collected, and subsequent sample preparation for TEM was performed by Wuhan Servicebio Biotechnology Co Ltd., which provided technical support. TEM images were analyzed under the guidance of electron microscope technology experts to observe the state of EA.hy926 endothelial cells and the morphological alterations in organelles.

Detection of mitochondrial membrane potential by JC-1 staining and flow cytometry

Since the vector used to construct the recombinant lentivirus had a GFP group and spontaneous green fluorescence (conflicts with the JC-1 staining green fluorescence probe), the fresh culture supernatant of wild-type and ApoM-KO SMMC-7721 cells in the logarithmic growth phase was collected and incubated with EA.hy926 cells to observe whether the removal of ApoM affected mitochondrial membrane potential. EA.hy926 cells that were approximately 80% confluent in a 100 mm culture dish were digested, inoculated in a 12-well plate at a density of 5×10^4 /well, and cultured for 24 hours. The cells were divided into 4 groups: EA.hy926 cells incubated with SMMC-7721 cell supernatant for 24 hours, EA.hy926 cells incubated with ApoM-KO SMMC-7721 cell supernatant for 24 hours, EA.hy926 cells incubated with the supernatant of ApoM-KO SMMC-7721 cells for 12 hours and then treated with 20 nM RAPA for 12 hours, and EA.hy926 cells incubated with SMMC-7721 cell supernatant for 12 hours and then treated with 20 nM RAPA for 12 hours. A mitochondrial membrane potential detection kit (JC-

1; Solarbio, Beijing, China) was used, and fluorescein isothiocyanate (FITC) and phycoerythrin (PE) dual-channel flow cytometry (BD FACS Canto II; Becton, Dickinson, and Co., Franklin Lakes, NJ, USA) was used for analysis. The relative proportion of red and green fluorescence can be used to measure the proportion of mitochondrial depolarization.

Cell energy metabolism analysis

A Seahorse XFe-96 extracellular flux analyzer (Seahorse Bioscience, Billerica, MA, USA) was used according to the instructions to determine the oxygen consumption rate (OCR) and extracellular acidification rate (ECAR) in real time for untreated EA.hy926 cells, lentivirus-infected negative control cells, and ApoM-overexpressing EA.hy926 cells, thereby assessing mitochondrial function.

Statistical analysis

The data for mouse aorta en face stain area, protein expression, mitochondrial membrane potential ($\Delta\Psi_m$), and energy metabolism were expressed as the means \pm standard errors (SEM). All animals were included in the analysis, with no exclusions. The inclusion criteria were as follows: mice aged 6 weeks, weighing 18–22 g, and free from any obvious health issues (such as injuries, infections, or abnormal behavior). Throughout the experiment, no mice experienced unexpected deaths or severe health problems, so all mice were included in the final analysis. The statistical analysis was performed using GraphPad Prism version 6.0 (GraphPad Software, Inc., San Diego, CA, USA), and comparisons between the 2 groups were evaluated using the Mann-Whitney *U* test. The nonparametric Kruskal-Wallis test was used to compare lipid species and species richness among the 4 groups; statistical analysis of lipid data was performed using R4.0.2 (R core team, Vienna, Austria), and *P* values for each lipid species between groups were calculated. The difference was considered statistically significant when *P* < 0.05.

Results

ApoM deficiency induced atherosclerosis and mitochondrial impairment in aortic endothelial cells of mice on an HFD

The mice were sampled according to the conventional method (Figure 1A). Generally, white plaques were observed in the aortas of ApoM-deficient mice fed an HFD (Figure 1B). En face staining of the aortas and Masson's trichrome

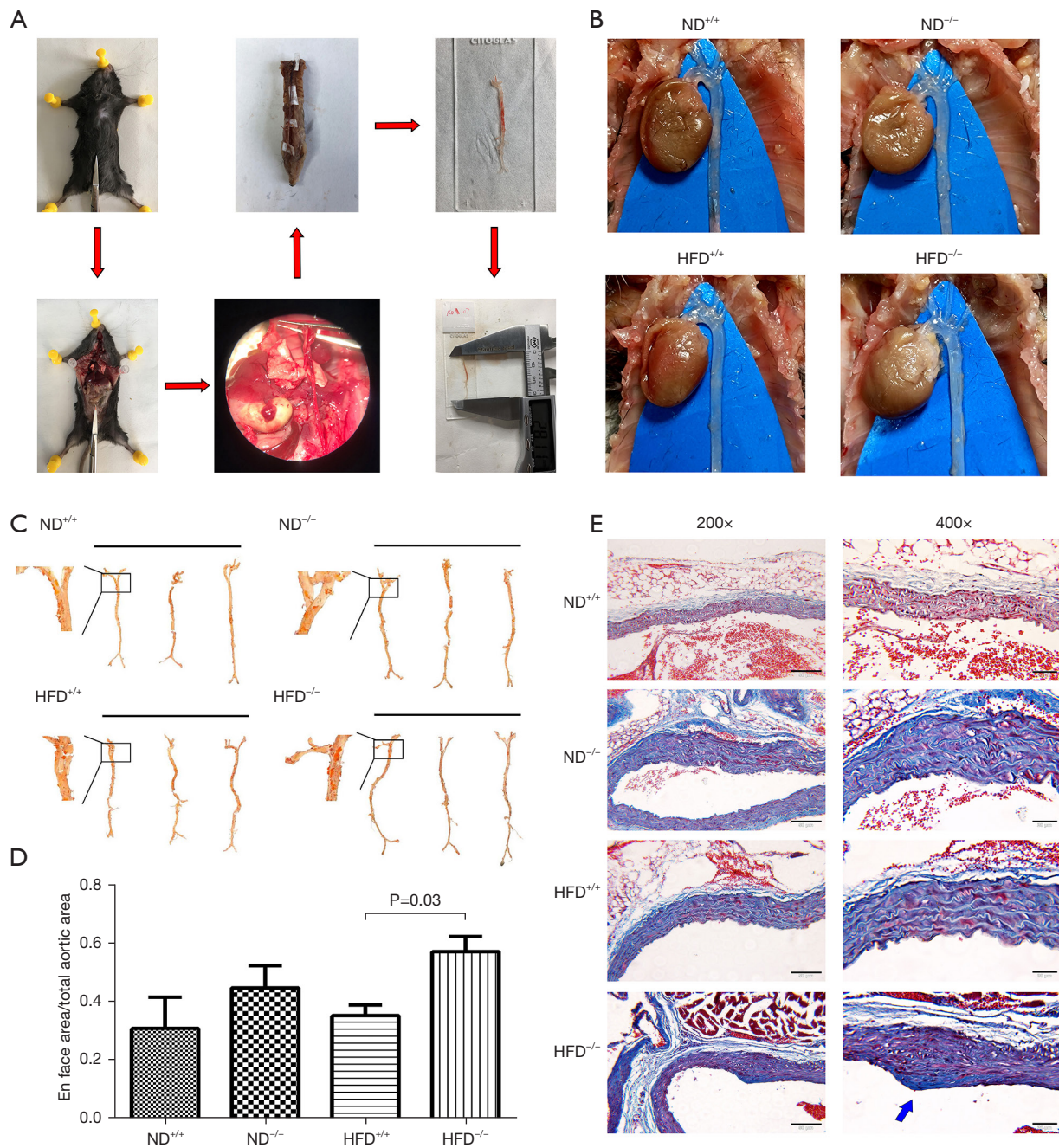


Figure 1 Lipid accumulation in aortas of *ApoM*^{-/-} mice fed a high-fat diet. (A) The process of sampling and fixation of the mouse aorta. (B) Macroscopic photographs of mouse aortas. (C) En face staining of mouse aortas. (D) Histogram of the ratio of the area of red deposits in the aorta divided by the total area of the lumen in the aorta in each group. The results are expressed as the means ± SEMs (mice n=6). (E) Masson trichrome staining of mouse aortic roots. The blue arrow points to a plaque of collagen fibers. The scale of the left image is 50 μm. Magnification: 200x. The right image is a partially enlarged view of the left image, and the scale is 20 μm. Magnification: 400x. ND^{+/+} represents the ND group of *ApoM*^{+/+} mice, ND^{-/-} represents the ND group of *ApoM*^{-/-} mice, HFD^{+/+} represents the *ApoM*^{+/+} mice HFD group, and HFD^{-/-} represents the *ApoM*^{-/-} mice HFD group. ApoM, apolipoprotein M; HFD, high-fat diet; ND, normal diet; SEMs, standard errors of the mean.

staining of collagen fibers in the aortic root showed that *ApoM*^{-/-} mice fed an HFD exhibited aortic lipid deposition and fibrosis, indicating successful establishment of an atherosclerotic model in the early stage of plaque formation (Figure 1C-1E). As shown in Figure 1C,1D, oil red O-positive staining was found in the aortic intima in each group, and the ratio of the positive staining area was slightly increased in *ApoM*^{-/-} mice compared with *ApoM*^{+/+} mice (fed an ND for 6 months) (P=0.32). However, the ratio of the positive staining area in *ApoM*^{-/-} mice was significantly higher than that in *ApoM*^{+/+} mice (fed an HFD for 6 months) (P=0.03). These results suggested that ApoM deficiency could lead to the exacerbation of lipid deposition in the aortic intima, and that an HFD could further aggravate this effect. Therefore, *ApoM*^{-/-} mice fed an HFD could serve as a research model for our subsequent experiments.

Masson's trichrome staining revealed that the collagen fibers in the aortic roots of *ApoM*^{+/+} mice fed an ND were blue-stained, muscle fibers were red-stained, and the fibers were arranged in an orderly fashion, indicating normal vascular morphology. In *ApoM*^{-/-} mice fed an ND and *ApoM*^{+/+} mice fed an HFD, the collagen fibers in the aortic root and the thickness of the vascular wall were increased. The aortic root collagen fibers of HFD-fed *ApoM*^{-/-} mice exhibited increased thickening, disordered arrangement, and visible collagen fiber plaques (blue block-shaped bump), and this group had the most serious fibrosis (Figure 1E). These findings suggested that aortic root fibrosis in *ApoM*^{-/-} mice fed an HFD was more severe than that in *ApoM*^{+/+} mice, the intima remained intact, and the formation of atherosclerotic plaques was in the early stage.

As shown in Figure 2, TEM image analysis showed that the morphology of the aorta and endothelial cells in *ApoM*^{+/+} mice fed an ND was essentially normal. In contrast, the aortic endothelial cells of *ApoM*^{-/-} mice exhibited signs of damage when compared to those of *ApoM*^{+/+} mice. The mitochondria within these cells appeared swollen, and their number decreased. These findings suggested that ApoM deficiency could potentially impair aortic endothelial cells and mitochondria.

The aortic endothelial cells of *ApoM*^{-/-} mice exhibited more severe damage compared to those of *ApoM*^{+/+} mice, with significantly swollen mitochondria, and a decreased number of these organelles. The impairment of aortic endothelial cells and mitochondria was more pronounced in HFD mice than in their isogenic ND counterparts, and *ApoM*^{-/-} mice fed an HFD displayed the most severe damage. These findings suggest that ApoM deficiency

may contribute to damage of aortic endothelial cells and mitochondria and this effect may be exacerbated by the consumption of an HFD.

Lipidomics analysis showed abnormal lipid metabolism, particularly aberrant expression of LBPA and acylcarnitine, in *ApoM*^{-/-} mice

Lipidomics analysis showed that in response to ApoM deficiency and HFD, serum levels of fatty acids and their metabolites (FFA, acylcarnitine), phospholipids (LPA, LPC, PC, PI, PS, plasmalogen PC), and sphingolipids [SM, Sph, GM3 (ganglioside), LacCer (lactose ceramide)] were significantly different (Figure 3A,3B). The levels of FFA, PI, and Sph in the livers of mice were also significantly different, as were those of GluCer, PA, PE, PG, PS, and S1P in the livers of mice (Figure 3C,3D). More data on individual lipids in polar lipids are provided in the supplementary material (Figures S1,S2). The level of serum acylcarnitine in *ApoM*^{-/-} mice fed an ND tended to be higher than that in *ApoM*^{+/+} mice, and the level of serum acylcarnitine in *ApoM*^{-/-} mice fed an HFD was significantly higher than that in *ApoM*^{+/+} mice (Figure 3B). We also examined the serum lipids of *ApoM*^{-/-} mice fed an ND for 12 months and found that all subtypes of acylcarnitine were significantly higher than those in *ApoM*^{+/+} mice (21). Acylcarnitine is a reliable marker of mitochondrial overload and incomplete fatty acid oxidation (26). However, in this study, acylcarnitine was not detected in the liver, which may be due to the extraction or detection method. LBPA is a class of unconventional anionic phospholipids specifically located in endosomes and the lysosomal inner membrane, and its expression is related to lysosomal function. We carefully reanalyzed the lipidomics data of ApoM-KO SMMC-7721 cells published in our previous paper (21) and found that the total amount and most subclasses of LBPA were significantly decreased in ApoM-deficient cells (Figure S3A-S3C). Upon examining the serum lipids of *ApoM*^{-/-} mice, a separate reanalysis revealed that ApoM deficiency resulted in a significant decrease in LBPA levels (Figure S3D). However, in this study, there was no significant difference in serum and liver levels of LBPA, which was different from the previous results. It may be that the feeding time and HFD affected the levels of LBPA.

Mitochondrial impairment induced by ApoM deficiency may be associated with compromised autophagy

The construction of the EA.hy926 cell model with

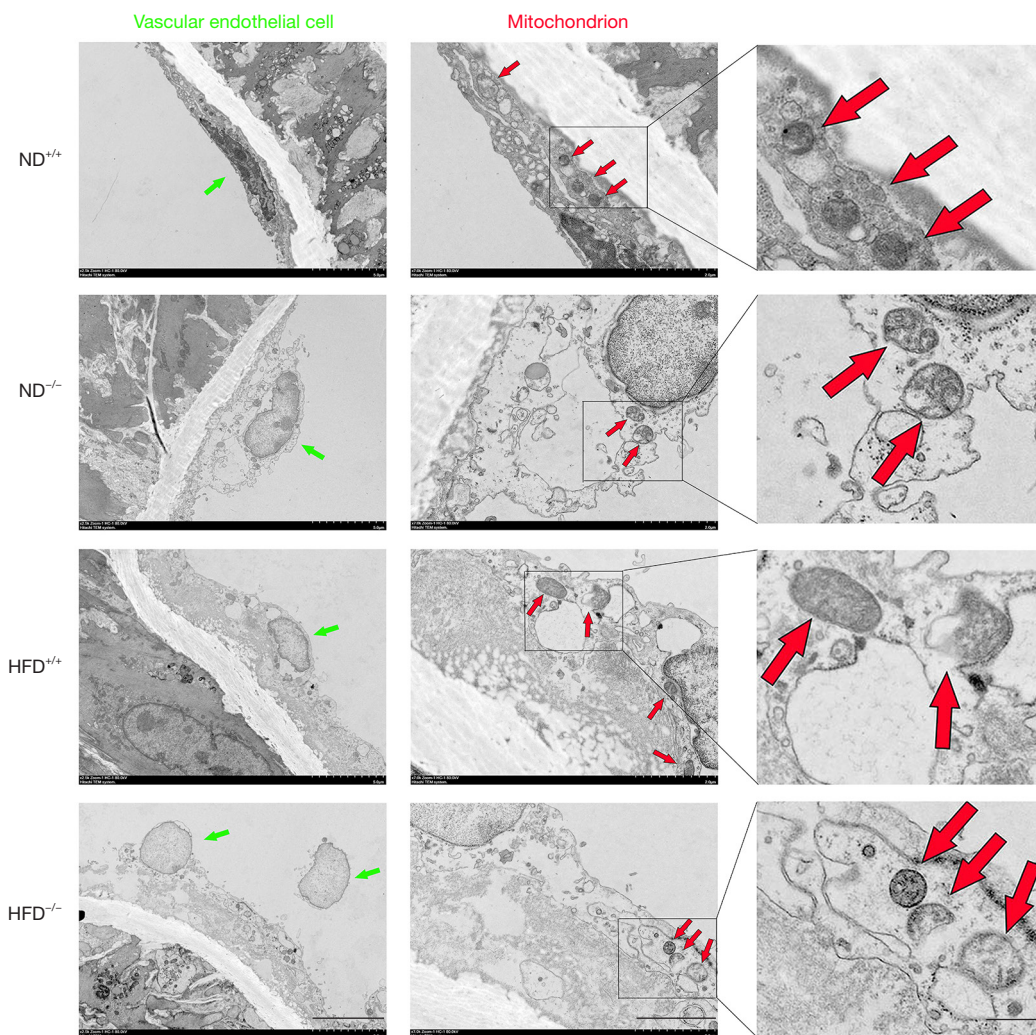
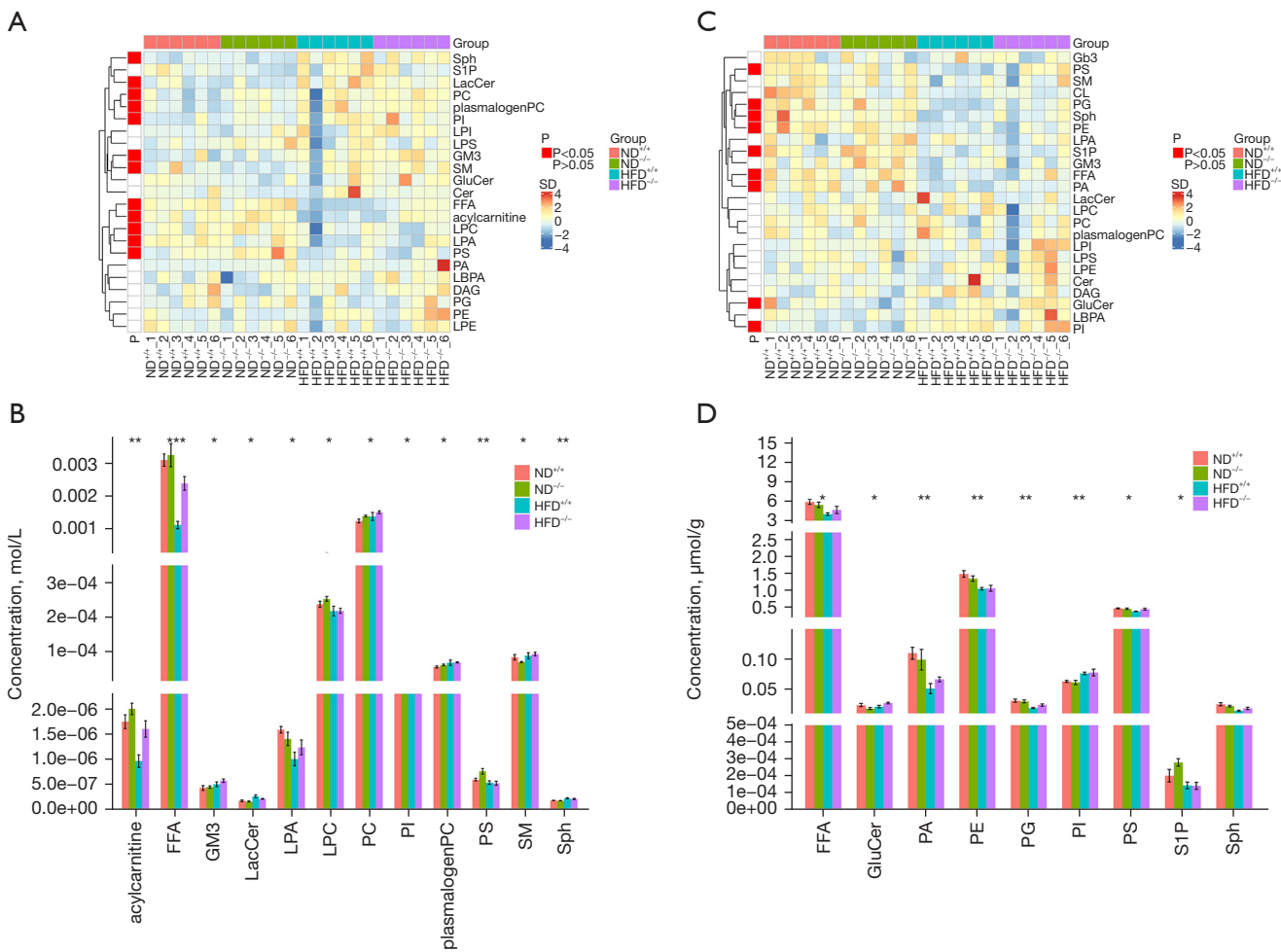


Figure 2 ApoM deficiency causes aortic, endothelial, and mitochondrial damage. Transmission electron micrograph of aortas. The green arrows point to endothelial cells in the aorta, and the red arrows point to mitochondria in endothelial cells. The scale of the left image is 5.0 μm . Magnification: 2,500 \times . The middle image is a partially enlarged view of the left image, and the scale is 2.0 μm . Magnification: 7,000 \times . The right image is a partially enlarged view of the middle image, and the scale is 0.5 μm . Magnification: 20,000 \times . ND^{+/+} represents the ND group of *ApoM*^{+/+} mice, ND^{-/-} represents the ND group of *ApoM*^{-/-} mice, HFD^{+/+} represents the *ApoM*^{+/+} mice HFD group, and HFD^{-/-} represents the *ApoM*^{-/-} mice HFD group. ApoM, apolipoprotein M; HFD, high-fat diet; ND, normal diet.

overexpressed ApoM has been successfully completed (Figure S4). Western blot analysis showed that the relative expression of LC3BII in EA.hy926 cells overexpressing ApoM was significantly increased (Figure 4A,4B; $P=0.002$), and the relative expression of P62 was significantly decreased (Figure 4C; $P=0.01$). During autophagy, cytoplasmic LC3BI is cleaved and conjugated to phosphatidylethanolamine to form lipidated LC3BII, which is recruited to the autophagosomal membrane, and the increase in LC3BII represents the induction of autophagy. P62, an autophagy

substrate, can be degraded by autophagy, and the decline in P62 levels reflects an increase in autophagic flux. The increased expression of LC3BII and decreased expression of P62 upon ApoM overexpression indicated that autophagic flux was enhanced and unobstructed.

Autophagy in EA.hy926 cells was modulated by autophagy agonist RAPA and autophagy inhibitor 3-MA, and the changes in mitochondrial morphology were observed by TEM. The ultrastructure of untreated EA.hy926 cells showed normal cell morphology, autophagic lysosomes, and



mitochondrial structure and quantity (Figure 4D). Edema and autophagic lysosome structures were observed in both types of lentivirus-infected cells, with more autophagic lysosome structures exhibiting double membrane structures in EA.hy926 cells overexpressing ApoM compared to negative control cells. Mitochondrial swelling and abnormal

cristae were observed in both lentivirus-infected cell lines. Compared to negative control cells (Figure 4E), the organelles in EA.hy926 cells overexpressing ApoM appeared slightly damaged, and the number of mitochondria were increased (Figure 4F). These findings suggested that ApoM overexpression could enhance autophagy and ameliorate

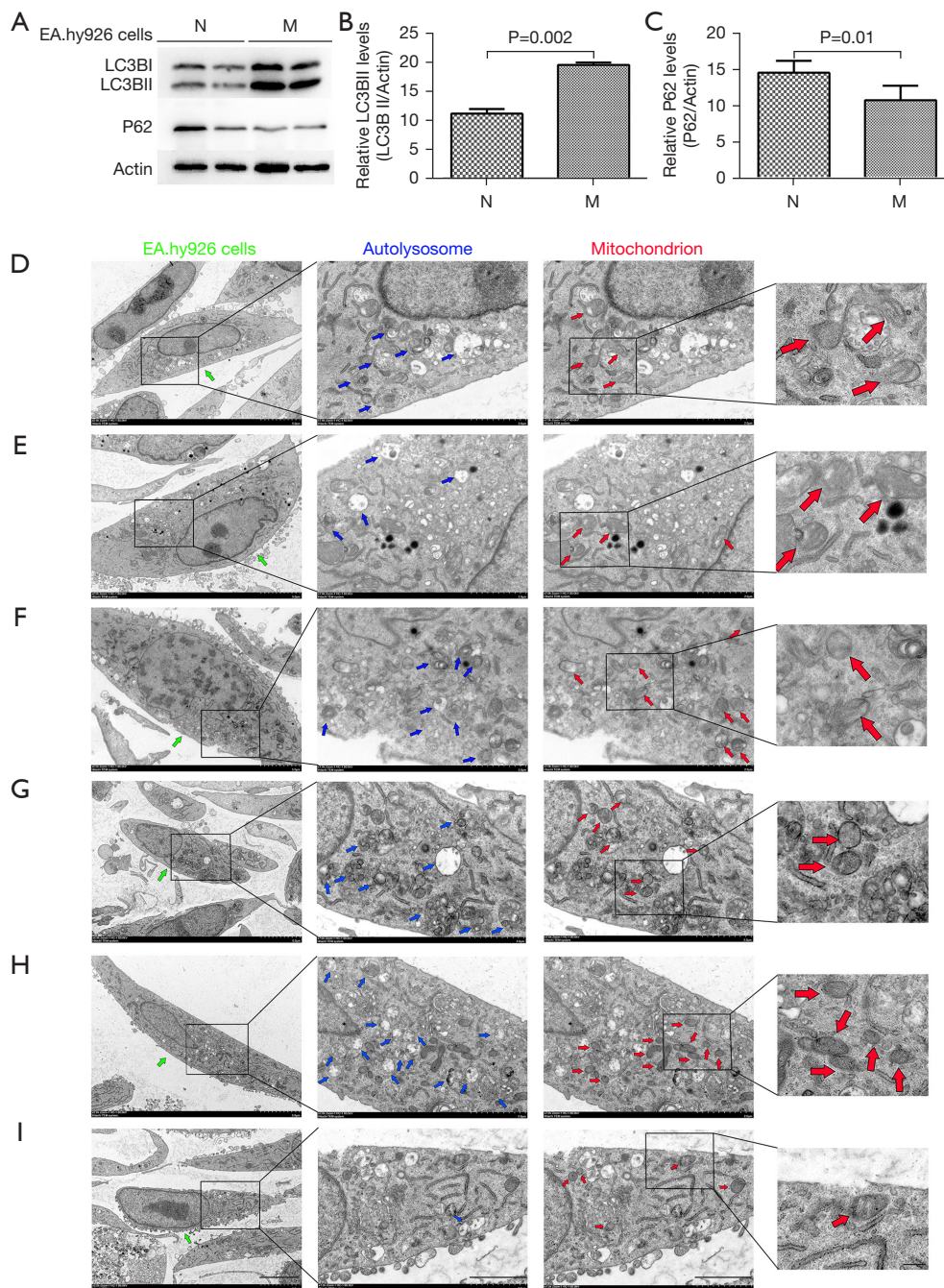


Figure 4 ApoM overexpression can enhance autophagy and improve mitochondrial structure in EA.hy926 cells. (A) Western blots. (B) LC3BII levels. (C) P62 levels. (D-I) Cell ultrastructure, as shown by TEM. (D) Untreated EA.hy926 cells. (E) Negative control EA.hy926 cells infected with the empty lentivirus. (F) EA.hy926 cells overexpressing ApoM. (G) Negative control EA.hy926 cells treated with RAPA. (H) EA.hy926 cells overexpressing ApoM treated with RAPA. (I) EA.hy926 cells overexpressing ApoM treated with 3-MA. The green arrows indicate EA.hy926 cells, the blue arrows indicate autolysosomes, and the red arrows indicate mitochondria in endothelial cells. The scale of the EA.hy926 cells image is 5.0 μm . Magnification: 2,500 \times . The autolysosome and mitochondria image is a partially enlarged view of the EA.hy926 cells image, and the scale is 2.0 μm . Magnification: 7,000 \times . The right image is a partially enlarged view of the mitochondria image, and the scale is 2.0 μm . Magnification: 17,500 \times . N represents negative control group of EA.hy926 cells, M represents overexpressing ApoM group of EA.hy926 cells. ApoM, apolipoprotein M; RAPA, rapamycin; TEM, transmission electron microscopy.

mitochondrial structure integrity.

Upon treatment with RAPA, the number of autophagic lysosomes in negative control cells increased significantly, and mitochondria swelling was alleviated (*Figure 4G*). After RAPA treatment, EA.hy926 cells overexpressing ApoM exhibited a remarkable increase in autophagic lysosomes, with mitochondria displaying minimal swelling, uniform size, and overall healthy cellular morphology (*Figure 4H*). However, when treated with 3-MA, EA.hy926 cells overexpressing ApoM showed a significant reduction in autophagic lysosomes, accompanied by swollen mitochondria and cellular distension (*Figure 4I*). These results suggested that ApoM overexpression enhanced autophagy activity in EA.hy926 cells, leading to reduced mitochondrial damage compared to negative control cells. Following RAPA treatment, the number of autophagic lysosomes further increased, and the structure of mitochondria remained largely intact.

The mitochondrial membrane potential ($\Delta\Psi_m$) of EA.hy926 cells was evaluated using the membrane potential-sensitive dye JC-1. The mitochondrial membrane potential ($\Delta\Psi_m$) is expressed as the ratio of red fluorescence (corresponding to mitochondria under oxidative stress) to green fluorescence (corresponding to mitochondria with less oxidative stress) (27). The red/green fluorescence ratio of EA.hy926 cells incubated with the supernatant of ApoM-KO SMMC-7721 cells was higher than that of wild-type SMMC-7721 cells (*Figure 5A, 5B*; $P=0.002$). However, the addition of 20 nM RAPA (autophagy agonist) to the supernatant of ApoM-KO SMMC-7721 cells significantly decreased the red/green fluorescence ratio of EA.hy926 cells ($P<0.001$). The red/green fluorescence of EA.hy926 cells was significantly reduced ($P=0.01$) when RAPA was added to the supernatant of wild-type SMMC-7721 cells. These results suggested that ApoM deletion could increase the red/green fluorescence ratio of EA.hy926 cells, indicating mitochondrial oxidative stress. When autophagy was induced, the red/green fluorescence ratio decreased, suggesting that the mitochondria had returned to normal state.

Next, we employed a Seahorse XFe-96 extracellular flux analyzer to investigate mitochondrial function and energy metabolism in EA.hy926 cells. OCR analysis showed that basal respiration ($P=0.006$) and adenosine triphosphate (ATP) production ($P=0.007$) were significantly diminished in ApoM-overexpressing EA.hy926 cells compared to negative control cells, whereas no significant alteration was observed in maximal mitochondrial respiration (*Figure 5C*).

Conversely, ApoM-overexpressing EA.hy926 cells showed elevated levels of non-mitochondrial respiration ($P=0.05$). The glycolytic stress assays demonstrated that glycolysis in negative control cells surpassed that in wild-type cells ($P=0.045$), whereas no significant changes were detected in glycolysis, glycolytic capacity, or glycolytic reserves in the other cells (*Figure 5D*).

Discussion

Atherosclerosis is a kind of progressive vascular disease that is caused by multiple factors. The pathophysiological features include thickening and hardening of the arterial wall, loss of elasticity, and stenosis of the lumen. The initial link between its initiation and development is injury and dysfunction in vascular endothelial cells (28). The mitochondria of vascular cells are involved in the regulation of vascular tone, angiogenesis, and the phenotype of vascular smooth muscle cells. Mitochondrial dysfunction can also lead to vascular pathologies such as atherosclerosis (29). Studies have shown that abnormal expression of ApoM is closely related to the occurrence and development of atherosclerosis, but the specific mechanism is not entirely clear, and a previous study focused on the cellular level and *Ldlr*^{-/-} mice (10). To date, our research group has not examined reports that directly observed the occurrence of atherosclerosis in ApoM-knockout mice, and whether ApoM is involved in cardiovascular diseases, especially whether the occurrence of atherosclerosis is related to the mitochondrial pathway, has not been reported. We have successfully established ApoM-knockout mice, and this study utilized a long-term high-fat feeding method to induce atherosclerosis and observe the role of ApoM in atherosclerosis and the possible mechanism. Additionally, the mechanism was further explored in EA.hy926 endothelial cells overexpressing ApoM. We found that *ApoM*^{-/-} mice exhibited more severe lipid deposition than *ApoM*^{+/+} mice in the aorta in response to an HFD. Aortic root fibrosis was obvious, the aortic intima remained intact, and atherosclerosis had developed, indicating an early stage. This period is the critical time for endothelial cell autophagy during atherosclerotic plaque progression and is the most vulnerable stage associated with mitochondrial damage (30). We also found that the aortic endothelial cells of *ApoM*^{-/-} mice were edematous, and the mitochondria in these cells were markedly swollen and structurally damaged.

Acylcarnitines are reliable markers of mitochondrial overload and incomplete fatty acid oxidation (24,26). Pei

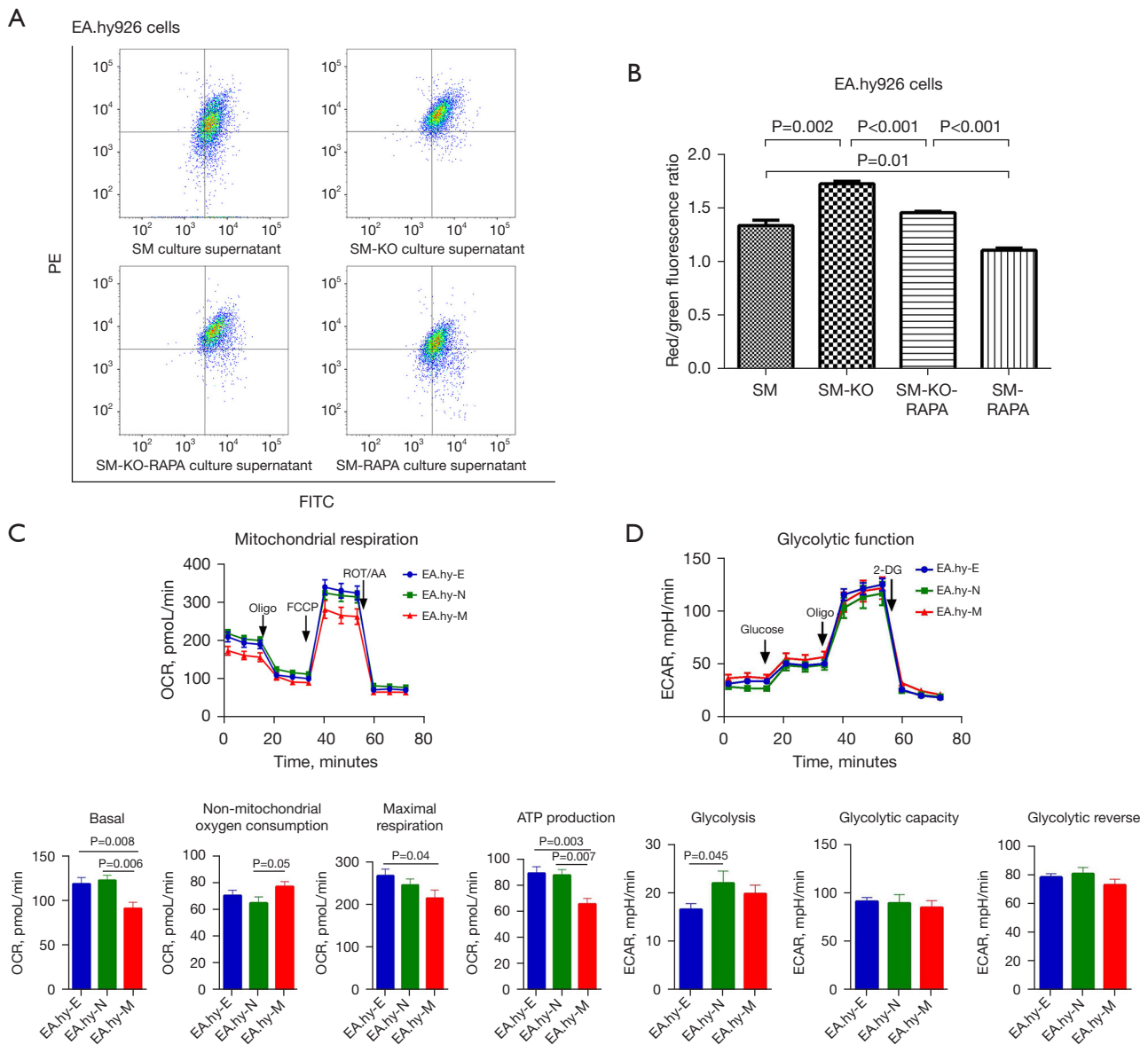


Figure 5 Effects of ApoM on mitochondrial membrane potential ($\Delta\Psi_m$) and energy metabolism in EA.hy926 cells. (A) Flow cytometry histogram. (B) Red/green fluorescence ratio histogram. (C) OCR. (D) Extracellular acidification rate (ECAR). SM, EA.hy926 cells incubated with SMMC-7721 cell supernatant for 24 h; SM-KO, EA.hy926 cells incubated with ApoM-KO SMMC-7721 cell supernatant for 24 h; SM-KO-RAPA, EA.hy926 cells incubated with the supernatant of ApoM-KO SMMC-7721 cells for 12 h, then treated with 20 nm RAPA for 12 h; SM-RAPA, EA.hy926 cells incubated with SMMC-7721 cell supernatant for 12 h, then treated with 20 nm RAPA for 12 h. ApoM, apolipoprotein M; ATP, adenosine triphosphate; EA.hy-E, untreated EA.hy926 cells; EA.hy-N, lentivirus-infected negative control cells; EA.hy-M, ApoM-overexpressing EA.hy926 cells. OCR, oxygen consumption rate; RAPA, rapamycin.

et al. (20) found that abnormal changes in mitochondrial damage and endoplasmic reticulum stress occurred in *ApoM*^{-/-} mouse kidneys, and deletion of the *ApoM* gene could increase apoptosis in mouse kidney tissue and mesangial cells through mitochondrial and endoplasmic

reticulum pathways. LBPA is a major component of the endosomal membrane and lysosomal inner membrane and has not been identified outside the endosomal and lysosomal membranes of cells (31). LBPA participates in protein and lipid transport through the late endosome and

serves as a characteristic marker of the autophagic lysosome degradation pathway (32). Lipidomics analysis revealed alterations in the expression of acylcarnitine and LBPA, which captured our attention. We observed an increase in serum acylcarnitine levels in *ApoM*^{-/-} mice fed an HFD. Moreover, we showed that the serum acylcarnitines in *ApoM*^{-/-} mice fed an ND for 12 months were increased from C14 to C18 (21). It was shown in a previous article that acylcarnitine is associated with the development of atherosclerosis (33), which may suggest that *ApoM*^{-/-} mice are inherently more susceptible to atherosclerosis. Increased accumulation of acylcarnitine, a lipid metabolite, suggests potential damage to mitochondrial lipid metabolism in *ApoM*^{-/-} mice (34). Our analysis revealed that deletion of *ApoM* resulted in a significant decrease in the total amount and most subclasses of LBPA. These findings suggest that *ApoM* deficiency may disrupt the autophagy-lysosome pathway and lead to a reduction in autophagy-lysosome formation. Zhang *et al.* (13) also observed abnormal expression of key proteins related to autophagy in the liver of *ApoM*-deficient mice and AML12 cells, providing further support for our hypothesis.

Next, we found that EA.hy926 cells overexpressing *ApoM* had better organelle structure than control cells, and the mitochondria and autophagic lysosomes were increased. LC3BII levels in EA.hy926 cells overexpressing *ApoM* were significantly increased, and P62 levels were significantly decreased, suggesting that *ApoM* could enhance autophagic flux. Autophagy can reduce the toxic accumulation of abnormal proteins and damaged organelles (especially mitochondria), inhibit oxidative stress and dysfunction, promote cell survival in harmful environments (35), and protect endothelial cells and platelets (36). A study has shown that *ApoM* is closely associated with S1P and exerts protective effects on vascular endothelial cells by binding to the S1P1 receptor (12). Our previous research demonstrated that EA.hy926 endothelial cells overexpressing *ApoM* exhibit high expression of the S1P1 receptor (25). Additionally, S1P is closely linked to mitochondrial function (37), as the S1P-S1P1 receptor axis can influence mitophagy. We hypothesized that *ApoM* could inhibit atherosclerosis by protecting mitochondrial structure and function, and this process may be related to autophagy-lysosomal pathway activation and mediated through the S1P-S1P1 receptor axis. *ApoM* is a secretory protein that typically does not directly participate in maintaining mitochondrial function. We hypothesize that highly expressed *ApoM* is secreted out of the cell, altering the state of S1P, which then stabilizes or

remains in the vicinity of the cell. Consequently, S1P acts as an intermediary substance, mediating the effect of *ApoM* on mitochondrial function through binding to S1P receptors on the cell membrane (Figure 6). Then, we observed the status of mitochondria by regulating the level of autophagy in endothelial cells.

The autophagy activator RAPA is a compound with a triene macrolide structure and is a potent and specific mTOR pathway blocker (38). 3-MA is a selective inhibitor of PI3K that can inhibit the formation of autophagic bodies in the early stage of autophagy (39). After RAPA treatment, the ultrastructure of EA.hy926 cells overexpressing *ApoM* and control cells was examined by TEM; the results showed that the number of autophagic lysosomes increased significantly, and mitochondrial swelling decreased. In particular, the mitochondria of EA.hy926 cells overexpressing *ApoM* showed no obvious swelling, and the size was uniform. After 3-MA treatment, the number of autophagic lysosomes in EA.hy926 cells overexpressing *ApoM* decreased significantly, and the mitochondria were swollen. These results suggest that *ApoM* can protect mitochondrial morphology and structure through autophagy.

Mitochondria play a key role in maintaining cell homeostasis. Mitochondrial dysfunction can lead to decreased production of ATP and increased production of reactive oxygen species (ROS), which is considered one of the triggers of vascular endothelial injury. Endothelial cells mainly generate ATP for energy through the glycolysis pathway (40), and mitochondria provide a small amount of energy. The vascular endothelium is the primary barrier that protects the vascular system from damage, and mitochondrial dysfunction in endothelial cells is closely related to the development of atherosclerosis (41). To confirm our results, we measured the mitochondrial membrane potential and energy metabolism in cells and examined the impact of *ApoM* expression on mitochondrial function. Previous results had shown that *ApoM* may affect mitochondrial morphology through the autophagy pathway, so we further detected mitochondrial membrane potential ($\Delta\Psi_m$) after inducing autophagy. Mitochondrial membrane potential ($\Delta\Psi_m$) can reflect the functional state of mitochondria to a certain extent because the carrier in lentivirus-infected cells expresses GFP, which conflicts with the detection of the membrane osmotic potential dye JC-1, and because *ApoM* is a secretory protein. Therefore, we incubated EA.hy926 cells (with low expression of *ApoM*) with the fresh culture supernatants of SMMC-7721 cells (with high expression of *ApoM*) and *ApoM*-

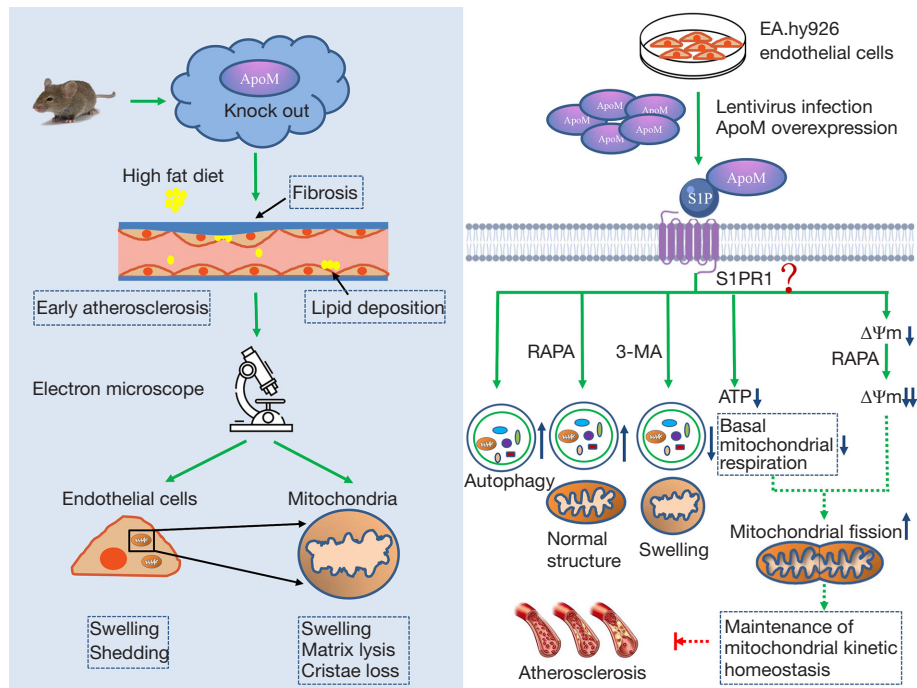


Figure 6 Schematic illustration of the experimental procedures and the hypothesized mechanism by which ApoM inhibits atherosclerosis by regulating autophagy and mitochondrial function. ApoM, apolipoprotein M; ATP, adenosine triphosphate; RAPA, rapamycin.

KO SMMC-7721 cells (without expression of ApoM) and induced autophagy with RAPA. The results showed that the mitochondrial membrane potential ($\Delta\Psi_m$) of EA.hy926 cells treated with ApoM-free supernatant was higher than that of cells treated with ApoM-containing supernatant. After the addition of 20 nM RAPA (autophagy agonist), the mitochondrial membrane potential ($\Delta\Psi_m$) decreased significantly. The mitochondrial membrane potential ($\Delta\Psi_m$) was further decreased after RAPA was added to supernatant containing ApoM. These findings suggested that ApoM and RAPA act in the same manner. Wang *et al.* (42) suggested that the decrease in mitochondrial membrane potential is one of the characteristics of mitochondrial dysfunction and is related to apoptosis. However, it has also been shown that in EA.hy926 cells, the red/green fluorescence ratio indicates the mitochondrial membrane potential, which is the ratio of mitochondria with oxidative stress and mitochondria with less oxidative stress (27). The results suggested that ApoM deletion could induce mitochondrial oxidative stress, and mitochondria returned to normal after autophagy induction. Therefore, ApoM may reduce endothelial mitochondrial oxidative stress through autophagy.

In our previous study, an energy metabolism experiment showed that basal and maximal mitochondrial respiration

and ATP production were dramatically decreased and nonmitochondrial respiration was significantly increased in ApoM-KO SMCC-7721 cells compared with wild-type SMCC-7721 cells, suggesting that mitochondrial oxidative stress was enhanced and oxidative phosphorylation was blocked in ApoM-KO SMCC-7721 cells (21). The results of glycolytic stress experiments demonstrated that the reduction in glycolysis, glycolytic capacity, and glycolysis reserve in liver cells could be partially attributed to the increase in mitochondrial oxidative stress after ApoM deletion (21). Surprisingly, EA.hy926 cells overexpressing ApoM showed no significant changes in maximal mitochondrial respiration, glycolysis, glycolytic capacity, or glycolytic reserves, but showed a significant decrease in basal mitochondrial respiration and ATP production compared with the negative control. In this study, EA.hy926 cells overexpressing ApoM showed better morphology under the microscope, and TEM showed that the number of mitochondria was increased and edema was reduced. The different effects of ApoM on mitochondrial respiration in the 2 cell lines may be due to the strong energy metabolism of liver cancer cells, and the main energy supply involves mitochondrial aerobic respiration, whereas the mitochondria of endothelial cells mainly

regulate vascular function, and the energy demand for mitochondria is relatively low and mainly involves glycolysis to produce ATP. It was found that more than three-quarters of ATP was synthesized by glycolysis in porcine endothelial cells cultured *in vitro*, and only a small amount of ATP was produced by mitochondria (43,44). A study (29) has shown that the mitochondria of vascular cells can regulate vascular tone, angiogenesis, and vascular smooth muscle cell phenotype. The mitochondria of vascular cells form a complex filamentous network, which is highly dynamic in morphology and distribution. Under well-oxygenated conditions, vascular cells exhibit abnormally high rates of glycolysis and rely on large amounts of ATP produced by glycolysis rather than mitochondrial oxidation to maintain their biological activity in the vasculature. Mitochondrial dysfunction can lead to vascular pathology such as atherosclerosis. In the physiological state, the mitochondrial dynamics of endothelial cells are in a stable dynamic balance to maintain the stability and function of mitochondria. After transient or long-term oxidative stress, human umbilical vein endothelial cells exhibit abnormal mitochondrial dynamics such as fusion and division, and the level of related factors will change, after which endothelial cell function will be impaired (45). A study (46) has shown that when the mitochondria of vascular endothelial cells divide, their mitochondrial membrane potential ($\Delta\Psi_m$), ATP production, and oxygen consumption decrease. This is consistent with what we observed in EA.hy926 cells overexpressing ApoM, suggesting that ApoM may protect endothelial cells by promoting mitochondrial fission to maintain the balance of mitochondrial dynamics. Thus, ApoM did not alter maximal mitochondrial respiration (reflecting maximal mitochondrial oxygen consumption) or glycolytic metabolism (the primary source of energy for endothelial cells) in EA.hy926 cells but decreased basal mitochondrial respiration and ATP production. Since low basal mitochondrial respiration is a normal physiological process in endothelial cells, this finding suggests that mitochondrial function is not affected, and ApoM may protect endothelial cells by maintaining low mitochondrial energy consumption.

There are still some limitations in this study that need to be further improved and studied. In the future, we will try to establish *ApoM*^{-/-} and *ApoM*^{+/+} mouse primary vascular endothelial cell models and ApoM-knockout endothelial cell lines. Moreover, multiple time points will be set in both cell and animal experiments to comprehensively and dynamically analyze mitochondrial function and autophagy levels, and to better understand the dynamic changes in

ApoM expression and function during the progress of atherosclerosis. We also considered collecting clinical atherosclerotic specimens with ethical approval to improve the study. Additionally, this study exclusively utilized male mice to control for potential hormonal variability that could influence metabolic processes and the development of atherosclerosis. However, in the context of ApoM and atherosclerosis, it remains necessary to include female individuals to explore potential gender differences.

In summary, this study mainly focused on the effect of ApoM on the mitochondrial function of endothelial cells and preliminarily showed that ApoM could protect autophagy and mitochondrial function during atherosclerosis, which provides an experimental basis for exploring the mechanism and therapeutic targets of atherosclerosis. Therefore, maintaining or elevating ApoM levels through lifestyle interventions and targeted drug delivery methods may be beneficial for vascular health. Meanwhile, we recognize the importance of measuring ApoM levels in health screenings. Exploring simple methods for quantifying ApoM, such as PCR and ELISA, will enhance its applicability in clinical settings. Regarding the deeper mechanism and the specific molecular pathways involved, further research is needed.

Conclusions

Our study highlights the critical role of ApoM in regulating atherosclerosis progression by modulating mitochondrial dynamics, autophagy, and lipid metabolism. In *ApoM*^{-/-} mice fed an HFD, early atherosclerosis markers emerged, accompanied by mitochondrial damage and compromised autophagy in endothelial cells. Conversely, ApoM overexpression in cells enhanced autophagic activity and mitochondrial resilience, while favoring mitochondrial fission and glycolytic metabolism. These findings suggest that ApoM-targeted therapies could safeguard mitochondrial health, improve autophagy, and maintain lipid homeostasis, thereby mitigating atherosclerosis risk.

Acknowledgments

We would like to thank Jian Shi and Bowen Li for their excellent technical assistance on flow cytometry and statistical analysis.

Footnote

Reporting Checklist: The authors have completed the

ARRIVE reporting checklist. Available at <https://cdt.amegroups.com/article/view/10.21037/cdt-2024-614/rc>

Data Sharing Statement: Available at <https://cdt.amegroups.com/article/view/10.21037/cdt-2024-614/dss>

Peer Review File: Available at <https://cdt.amegroups.com/article/view/10.21037/cdt-2024-614/prf>

Funding: This research was supported by Top Talent of Changzhou “The 14th Five-Year Plan” High-Level Health Talents Training Project (No. 2022260), and the International Cooperation Foundation of Changzhou (No. CZ20220024).

Conflicts of Interest: All authors have completed the ICMJE uniform disclosure form (available at <https://cdt.amegroups.com/article/view/10.21037/cdt-2024-614/coif>). B.J. is from Lipidall Technologies Company Limited, Changzhou, China. The other authors have no conflicts of interest to declare.

Ethical Statement: The authors are accountable for all aspects of the work in ensuring that questions related to the accuracy or integrity of any part of the work are appropriately investigated and resolved. The animal experiment was approved by the Ethics Committee of Soochow University. The experimental design and implementation plan of this study fully considered the principles of safety and fairness, as well as the requirements of animal welfare and national animal experiment management and ethics.

Open Access Statement: This is an Open Access article distributed in accordance with the Creative Commons Attribution-NonCommercial-NoDerivs 4.0 International License (CC BY-NC-ND 4.0), which permits the non-commercial replication and distribution of the article with the strict proviso that no changes or edits are made and the original work is properly cited (including links to both the formal publication through the relevant DOI and the license). See: <https://creativecommons.org/licenses/by-nc-nd/4.0/>.

References

- Burggraaf B, van Breukelen-van der Stoep DE, de Vries MA, et al. Progression of subclinical atherosclerosis in subjects with rheumatoid arthritis and the metabolic syndrome. *Atherosclerosis* 2018;271:84-91.
- Wang Y, Hu S, Ren L, et al. Lp-PLA(2) as a risk factor of early neurological deterioration in acute ischemic stroke with TOAST type of large arterial atherosclerosis. *Neurol Res* 2019;41:1-8.
- Geladari E, Tsamadia P, Vallianou NG. ANGPTL3 Inhibitors- Their Role in Cardiovascular Disease Through Regulation of Lipid Metabolism. *Circ J* 2019;83:267-73.
- Mocci G, Sukhvasi K, Örd T, et al. Single-Cell Gene-Regulatory Networks of Advanced Symptomatic Atherosclerosis. *Circ Res* 2024;134:1405-23.
- Marchio P, Guerra-Ojeda S, Vila JM, et al. Targeting Early Atherosclerosis: A Focus on Oxidative Stress and Inflammation. *Oxid Med Cell Longev* 2019;2019:8563845.
- Lu Y, Cui X, Zhang L, et al. The Functional Role of Lipoproteins in Atherosclerosis: Novel Directions for Diagnosis and Targeting Therapy. *Aging Dis* 2022;13:491-520.
- Xu N, Dahlbäck B. A novel human apolipoprotein (apoM). *J Biol Chem* 1999;274:31286-90.
- Hajny S, Christoffersen C. A Novel Perspective on the ApoM-S1P Axis, Highlighting the Metabolism of ApoM and Its Role in Liver Fibrosis and Neuroinflammation. *Int J Mol Sci* 2017;18:1636.
- Velagapudi S, Rohrer L, Poti F, et al. Apolipoprotein M and Sphingosine-1-Phosphate Receptor 1 Promote the Transendothelial Transport of High-Density Lipoprotein. *Arterioscler Thromb Vasc Biol* 2021;41:e468-79.
- Wolfrum C, Poy MN, Stoffel M. Apolipoprotein M is required for prebeta-HDL formation and cholesterol efflux to HDL and protects against atherosclerosis. *Nat Med* 2005;11:418-22.
- Christoffersen C, Jauhiainen M, Moser M, et al. Effect of apolipoprotein M on high density lipoprotein metabolism and atherosclerosis in low density lipoprotein receptor knock-out mice. *J Biol Chem* 2008;283:1839-47.
- Christoffersen C, Obinata H, Kumaraswamy SB, et al. Endothelium-protective sphingosine-1-phosphate provided by HDL-associated apolipoprotein M. *Proc Natl Acad Sci U S A* 2011;108:9613-8.
- Zhang X, Zhang P, Gao J, et al. Autophagy dysregulation caused by ApoM deficiency plays an important role in liver lipid metabolic disorder. *Biochem Biophys Res Commun* 2018;495:2643-8.
- Guo Z, Valenzuela Ripoll C, Picataggi A, et al. Apolipoprotein M Attenuates Anthracycline Cardiotoxicity and Lysosomal Injury. *JACC Basic Transl Sci* 2023;8:340-55.

15. Mizushima N. Autophagy: process and function. *Genes Dev* 2007;21:2861-73.
16. Wang J, Wang WN, Xu SB, et al. MicroRNA-214-3p: A link between autophagy and endothelial cell dysfunction in atherosclerosis. *Acta Physiol (Oxf)* 2018.
17. Xu H, Fu J, Tu Q, et al. The SGLT2 inhibitor empagliflozin attenuates atherosclerosis progression by inducing autophagy. *J Physiol Biochem* 2024;80:27-39.
18. Wang Z, Sun W, Zhang K, et al. New insights into the relationship of mitochondrial metabolism and atherosclerosis. *Cell Signal* 2025;127:111580.
19. Liu Z, Huang N, Liu C, et al. Mitochondrial DNA in atherosclerosis research progress: a mini review. *Front Immunol* 2025;16:1526390.
20. Pei W, Wu Y, Zhang X, et al. Deletion of ApoM gene induces apoptosis in mouse kidney via mitochondrial and endoplasmic reticulum stress pathways. *Biochem Biophys Res Commun* 2018;505:891-7.
21. Shi Y, Lam SM, Liu H, et al. Comprehensive lipidomics in apoM(-/-) mice reveals an overall state of metabolic distress and attenuated hepatic lipid secretion into the circulation. *J Genet Genomics* 2020;47:523-34.
22. Shi Y, Liu H, Liu H, et al. Increased expression levels of inflammatory cytokines and adhesion molecules in lipopolysaccharide-induced acute inflammatory apoM^{-/-} mice. *Mol Med Rep* 2020;22:3117-26.
23. Lam SM, Zhang C, Wang Z, et al. A multi-omics investigation of the composition and function of extracellular vesicles along the temporal trajectory of COVID-19. *Nat Metab* 2021;3:909-22.
24. Xia JG, Li B, Zhang H, et al. Precise Metabolomics Defines Systemic Metabolic Dysregulation Distinct to Acute Myocardial Infarction Associated With Diabetes. *Arterioscler Thromb Vasc Biol* 2023;43:581-96.
25. Shi Y, Liang Y, Zhang J, et al. Non-negligible factors in studying the ApoM-S1P axis using EA.hy926 cells. *Ann Transl Med* 2020;8:383.
26. Koves TR, Ussher JR, Noland RC, et al. Mitochondrial overload and incomplete fatty acid oxidation contribute to skeletal muscle insulin resistance. *Cell Metab* 2008;7:45-56.
27. Wu X, Jiang L, Sun X, et al. Mono(2-ethylhexyl) phthalate induces autophagy-dependent apoptosis through lysosomal-mitochondrial axis in human endothelial cells. *Food Chem Toxicol* 2017;106:273-82.
28. Wang K, Yang C, Shi J, et al. Ox-LDL-induced lncRNA MALAT1 promotes autophagy in human umbilical vein endothelial cells by sponging miR-216a-5p and regulating Beclin-1 expression. *Eur J Pharmacol* 2019;858:172338.
29. Zhang X, Gao F. Exercise improves vascular health: Role of mitochondria. *Free Radic Biol Med* 2021;177:347-59.
30. Ballinger SW, Patterson C, Knight-Lozano CA, et al. Mitochondrial integrity and function in atherogenesis. *Circulation* 2002;106:544-9.
31. Gruenberg J. Life in the lumen: The multivesicular endosome. *Traffic* 2020;21:76-93.
32. Matsuo H, Chevallier J, Mayran N, et al. Role of LBPA and Alix in multivesicular liposome formation and endosome organization. *Science* 2004;303:531-4.
33. Nakajima T, Fukuda T, Shibasaki I, et al. Pathophysiological roles of the serum acylcarnitine level and acylcarnitine/free carnitine ratio in patients with cardiovascular diseases. *Int J Cardiol Heart Vasc* 2024;51:101386.
34. Dunlop K, Sarr O, Stachura N, et al. Differential and Synergistic Effects of Low Birth Weight and Western Diet on Skeletal Muscle Vasculature, Mitochondrial Lipid Metabolism and Insulin Signaling in Male Guinea Pigs. *Nutrients* 2021;13:4315.
35. Livingston MJ, Wang J, Zhou J, et al. Clearance of damaged mitochondria via mitophagy is important to the protective effect of ischemic preconditioning in kidneys. *Autophagy* 2019;15:2142-62.
36. Carnevale R, Nocella C, Schiavon S, et al. Beneficial effects of a combination of natural product activators of autophagy on endothelial cells and platelets. *Br J Pharmacol* 2021;178:2146-59.
37. Duan M, Gao P, Chen SX, et al. Sphingosine-1-phosphate in mitochondrial function and metabolic diseases. *Obes Rev* 2022;23:e13426.
38. Panwar V, Singh A, Bhatt M, et al. Multifaceted role of mTOR (mammalian target of rapamycin) signaling pathway in human health and disease. *Signal Transduct Target Ther* 2023;8:375.
39. Wu YT, Tan HL, Shui G, et al. Dual role of 3-methyladenine in modulation of autophagy via different temporal patterns of inhibition on class I and III phosphoinositide 3-kinase. *J Biol Chem* 2010;285:10850-61.
40. Zhou H, Shi C, Hu S, et al. BI1 is associated with microvascular protection in cardiac ischemia reperfusion injury via repressing Syk-Nox2-Drp1-mitochondrial fission pathways. *Angiogenesis* 2018;21:599-615.
41. Tamargo IA, Baek KI, Kim Y, et al. Flow-induced reprogramming of endothelial cells in atherosclerosis. *Nat Rev Cardiol* 2023;20:738-53.
42. Wang P, Deng J, Dong J, et al. TDP-43 induces mitochondrial damage and activates the mitochondrial

- unfolded protein response. *PLoS Genet* 2019;15:e1007947.
43. Oldendorf WH, Cornford ME, Brown WJ. The large apparent work capability of the blood-brain barrier: a study of the mitochondrial content of capillary endothelial cells in brain and other tissues of the rat. *Ann Neurol* 1977;1:409-17.
 44. Culic O, Gruwel ML, Schrader J. Energy turnover of vascular endothelial cells. *Am J Physiol* 1997;273:C205-13.
 45. Jendrach M, Mai S, Pohl S, et al. Short- and long-term alterations of mitochondrial morphology, dynamics and mtDNA after transient oxidative stress. *Mitochondrion* 2008;8:293-304.
 46. Chiong M, Cartes-Saavedra B, Norambuena-Soto I, et al. Mitochondrial metabolism and the control of vascular smooth muscle cell proliferation. *Front Cell Dev Biol* 2014;2:72.

Cite this article as: Shi Y, Yao S, Jiang B, Zhang J, Cao M, Wu J, Zheng L, Xu N, Zhang X, Shui G, Luo G. Apolipoprotein M delays the development of atherosclerosis by regulating autophagy and mitochondrial function. *Cardiovasc Diagn Ther* 2025;15(2):423-440. doi: 10.21037/cdt-2024-614